Photographic Depiction of the Field of View with Spectacles-mounted Low Vision Aids

Jae-Hyun Jung, PhD, FAAO,[1]* Nish Mohith Kurukuti, BS,[1] and Eli Peli, MS, OD, FAAO[1]

SIGNIFICANCE: Photographic depiction helps to illustrate the primary and secondary field of view effects of low vision devices along with their utility to clinicians, patients, and caretakers. This technique may also be helpful for designers and researchers in improving the design and fitting of low vision devices.

PURPOSE: The field of view through spectacles-mounted low vision devices has typically been evaluated using perimetry. However, the perimetric field diagram is different from the retinal image and often fails to represent the important aspects of the field of view and visual parameters. We developed a photographic depiction method to record and veridically show the field of view effects of these devices.

METHODS: We used a 3D-printed holder to place spectacles-mounted devices at the same distance from the empirically determined reference point of the field of view in a camera lens ($f = 16$ mm) as they would be from an eye, when in use. The field of view effects of a bioptic telescope, a minifier (reverse telescope), and peripheral prisms were captured using a conventional camera, representing retinal images. The human eye pupil size (adjusting the *F* number: f/2.8 to f/8 and f/22 in the camera lens) and fitting parameters (pantoscopic tilt and back vertex distance) varied.

RESULTS: Real-world indoor and outdoor walking and driving scenarios were depicted as retinal images illustrating the field of view through low vision devices, distinguishing optical and obscuration scotomas, and demonstrating secondary effects (spatial distortions, viewpoint changes, diplopia, spurious reflection, and multiplexing effects) not illustrated by perimetric field diagrams.

CONCLUSIONS: Photographic depiction illustrates the primary and secondary field of view effects of the low vision devices. These images highlight the benefit and possible trade-offs of the low vision devices and may be beneficial in education and training.

Optom Vis Sci 2021;98:1210–1226. doi:10.1097/OPX.0000000000001790

Supplemental Digital Content: *Direct URL links are provided within the text.*

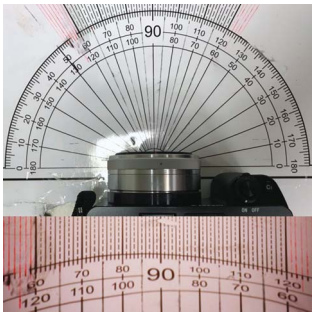

Author Affiliations:
[1]Schepens Eye Research Institute of Massachusetts Eye and Ear, Department of Ophthalmology, Harvard Medical School, Boston, Massachusetts
*jaehyun_jung@meei.harvard.edu

Spectacles-mounted visual aids including bioptic telescopes,[1–6] image minifiers (based on a reverse Galilean telescope),[7–11] and prisms[12–14] have been developed for low vision patients. All these devices modify the field of view, the portions of the area seen through the low vision devices that fall on the visual field (functioning portions of the retina),[15] and thus expand (image minifiers) or shift (prisms) the field of view, or enlarge the apparent size of the image (telescopes). Visualizing the effect of the low vision devices in terms of the field of view is necessary to understand and demonstrate the expected benefits and trade-offs of the devices to potential patients, caretakers, and clinicians.

The field of view through low vision devices has been traditionally evaluated with perimetry[9,11,13,16–18] and illustrated using a field diagram,[19,20] a map of the angular position of targets detected in the perimeter when the subject is looking at a fixation target (usually at the center of the perimeter).[18,21,22] The perimetric field diagram illustrates the field of view with the device in the perimeter (object) domain (the angular distance of visible targets from the fixation) but not in the retinal image domain (i.e., visual field). *Photographic depiction*: taking a picture through spectacles-mounted low vision devices using a camera, demonstrates the field of view, as a retinal image (subject's retinal eccentricity).

The angular size of the retinal image through the telescope or minifier is smaller or larger than without the device, respectively. A perimetric field diagram illustrates the field of view but does not veridically depict the angular size and location of the retinal image through the devices. For example, the field of view through the prism is shifted in the field diagram (Fig. 1A), but the location of the retinal image through the prism is not shifted.

Optical scotoma is another field of view effect illustrated differently in the field diagram and in the retinal image domain. Optical scotomas, such as jack-in-the-box scotoma with spectacles correction for aphakia,[24] bioptic ring scotoma,[25,26] and prismatic apical scotoma,[18,23] are measurable by perimetry and marked as nonseeing black/gray areas in the field diagram. The patient cannot detect objects that fall within the optical scotoma field, yet the scotomas are not perceived as black and do not appear explicitly in the retinal image. The optical scotoma may only be noticeable by the user as a discontinuation of image contents between the inside and outside of the device's aperture. The optical scotomas are different from *obscuration scotomas* caused by physical blocking,[14] such as the spectacles frame[27] or the body of the devices.[28] An obscuration scotoma is indeed observed as black (or the color of the obscuring object) and thus is seen similarly in both the field diagram and the

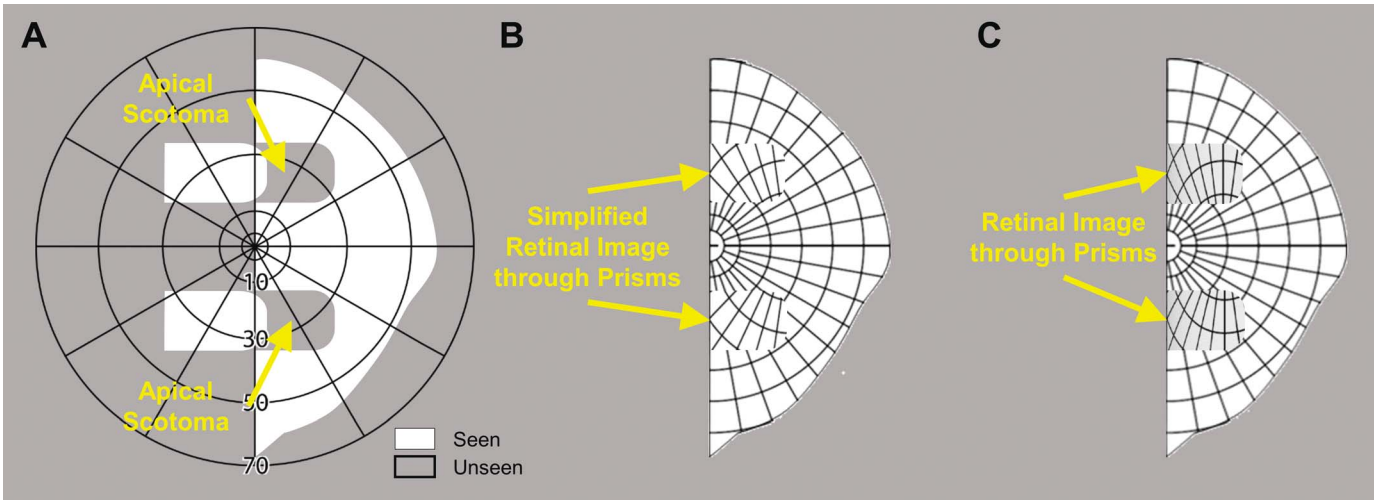

FIGURE 1. Field diagrams and percept diagrams. (A) Calculated monocular (left eye) field diagram of a patient with left homonymous hemianopia wearing 57Δ horizontal peripheral prisms. The field diagram illustrates two 30° wide by 20° high segments in the blind field (shifted view) made visible by the peripheral prism. The apical scotoma is also visible in the field diagram as unseen areas within the right, seeing, visual field. (B) Percept diagram (a calculated view of a polar perimetry grid observed by the patient through the device)[18] simulates the retinal image with the peripheral prisms. Apical scotoma is invisible here and only notable as discontinuity between views inside and outside the peripheral prisms. (C) Calculated percept diagram considering additional effects, such as distortions (minification) and dimming of the shifted view.[23]

retinal image. However, in the perimetric field diagram, the appearance of obscuration and optical scotomas is not distinguishable.[17,26] A method to illustrate the retinal image (patient's view) should distinguish the effects of the two different scotomas and their potential impact on the functionality of the low vision devices.

Diplopia (perceiving the same object in two different directions) is noticeable and bothersome to the user in actual use and thus should be avoided when fitting low vision devices (e.g., peripheral prisms[18] and image minifiers). Although diplopia is measurable in perimetry by asking the patient to report when it occurs,[21,23] it is missed in conventional perimetry unless the perimetrist is anticipating it and asks the patient to report it (not common practice). A method that illustrates the diplopia caused by devices on the retinal image would explicitly demonstrate that effect and could better guide testing and fitting. Apfelbaum et al.[15,18] introduced the percept diagram (Fig. 1B) to simulate the retinal image with low vision devices. A percept diagram illustrates what the world would look like on the retina if the world were a Goldmann polar grid. The percept diagram is calculated from the field diagram, inheriting some of the issues listed previously. Various field of view effects such as spatial distortion,[29,30] total internal and spurious reflections, dimming effects,[23] contrast reduction,[31,32] and diplopia are rarely measured in perimetry. Thus, the percept diagram does not illustrate those either (Fig. 1B). Even if some of these effects are considered with additional modeling (Fig. 1C),[23] the percept diagram still may not represent all the effects. For example, the percept diagram and most ray tracing computations assume a pinhole camera,[18,33] which ignores additional secondary effects such as blur (due to the proximity of the device to the eye), vignetting, and multiplexing effects (showing two different views superimposed [through and outside of the devices] at the boundary of the device)[34] due to the finite size of the physical pupil.

Few camera systems were previously developed to depict the scene through specific devices.[35–38] Tremblay et al.[35,36] implemented a customized human eye model and a relay optics system with a camera in the model's retinal plane to depict the retinal image magnified with their contact lens telescope. The system's high image quality enabled the evaluation of the device resolution, but the field of view (34.5°) was not wide enough to illustrate the field of view of the telescope, which is one of the scopes of our article.

Here, we use a commercial camera and a wide field of view lens selected to match the focal length and pupil size effects of the human eye. Simply taking a picture from behind a visual aid[7,11,17,18,25,39] does not provide an accurate representation of the field of view effects. Besides geometrical miscalibration, other camera settings are not matched with those of the human eye. We address such issues in this paper. Using the photographic depiction setup, the differences between the field of view effects on the perimetric field diagram and the retinal image from the photographic depiction in practical scenarios are illustrated and interpreted.

METHODS

Reference Point of Field of View in the Camera Lens

To correctly depict the field of view effects, the spectacles-mounted low vision devices should be located at the same distance from the reference point of the field of view in the camera system as the human eye. Without such correspondence, all angular relations to the devices, such as field of view, perspective, parallax, eccentricity, and angle of incidence and its consequences, would be incorrectly depicted and misrepresent the retinal image. In camera systems, the reference point for angular relations is the entrance pupil,[40,41] although the nodal point may be used under paraxial approximation.[7,18,23,42]

The distance from the reference point of the field of view in the camera system to the back vertex of the spectacles lens that carries the devices (reference-to-lens distance, *e*) should be matched with the distance in actual use (Fig. 2). Because the entrance pupil of the eye is located 4 mm behind the corneal front surface,[43] the spectacles lens should be located 4 mm farther than the back vertex distance from the reference point of the camera lens. We assume

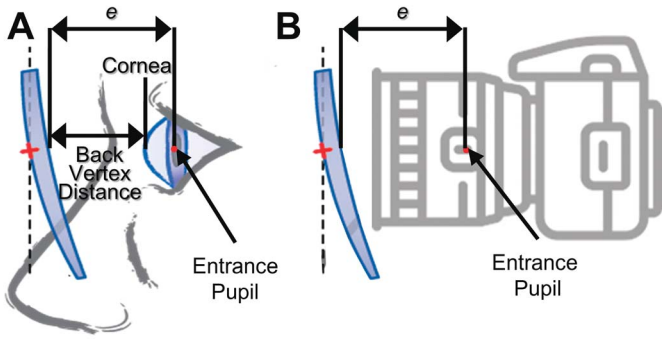

FIGURE 2. Matching the camera's reference-to-lens distance (*e*) with the human eye. (A) When a user wears a spectacles-mounted visual aid, the spectacles carrier lens is located approximately 17 mm in front of the eye's entrance pupil. (B) For angularly accurate photographic depiction, the spectacles should be mounted at the same reference-to-lens distance from the entrance pupil of the camera lens.

that the spectacles' back vertex distance is approximately 13 mm,[18] and thus, the reference-to-lens distance is approximately 17 mm. We also enabled varying the back vertex distance within a range of ±3 mm to evaluate the effects of individual variations (e.g., deeper or shallower eye or nose bridge structure).[44]

The reference point of the field of view in the camera lens, a specification that is not often released to the public, should be empirically determined to match the reference-to-lens distance with the human eye. In a typical camera lens, the entrance pupil is more than 20 mm behind the front surface of the camera lens, which makes it impossible to mount a visual aid at the human eye reference-to-lens distance (about 17 mm).

We used a mirrorless camera with a camera lens selected to match the scale of the focal length and aperture sizes with that of the human eye. We chose Sony (Tokyo, Japan) α6000 mirrorless camera (23.5 × 15.6 mm sensor with 6000 × 4000 resolution). This camera can accept a thin lens commonly known as a "pancake" lens (Sony SEL16F28) with an entrance pupil located closer than 17 mm from the lens front surface (16-mm focal length and maximum f/2.8) with a wide field of view (73 × 52°). The human eye has a 22 mm focal length and *F* number (ratio of the focal length and the pupil size) that ranges from f/2.1 in the dark to f/8.3 in the sunlight.[43] Because the human eye is filled with vitreous humor (refractive index of 1.34), the corresponding effective focal length of the human eye in the air is about the same as the focal length of the pancake camera lens we used (16 mm ≈ 22 mm/1.34). The range of *F* number in the human eye is fully covered by this lens.

To determine the reference point of the field of view in the camera lens, we used the perspective measurement. Whereas parallel railroad tracks appear to converge far from the eye or a camera image because of the perspective, diverging lines appear parallel to each other when the reference point of the perspective and the origin of the diverging lines are matched. We used large printed protractor lines (Appendix A, available at http://links.lww.com/OPX/A534) to measure the reference point in the camera lens, as proposed by Steptoe.[45]

3D-printed Holders for Spectacles-mounted Low Vision Devices

To match the reference-to-lens distance in the human eye and the camera system, we developed two types of holders for low vision devices (mounted on a lens blank or spectacles, respectively) using 3D printing. Both the lens blank holder and the spectacles frame holder are designed to fit on the outer surface of the pancake lens to keep the reference-to-lens distance at 17 mm and align the axes of the carrier lens and the camera lens. The camera lens center in the photographic depiction (optic axis and center pixel of the image) corresponds to the fovea of a human eye.

Fig. 3 shows the 3D-printed holder for an ophthalmic lens blank carrying the low vision devices. A bioptic Keplerian telescope (VES Mini 3×; Ocutech, Chapel Hill, NC; 14 mm in diameter) was mounted through the lens blank protruding 5 mm towards the eye, as is the standard fitting of that telescope.[46] To demonstrate the on-axis telescope in-use, we mounted the telescope at the optic axis of the lens blank (Figs. 3A, B). For the off-axis condition (when not in use), as the telescope is sitting most of the time, the telescope was mounted through the lens blank 8.5 mm above the lens optical center (10 mm below the eye wire of the spectacles lens) and tilted 10° up (Figs. 3D, E).[46] Similarly, the image minifier (Field Expander 0.6×; Ocutech; 13.5 mm in diameter) was mounted on-axis position with a 0.5-mm protrusion towards the eye (Fig. 3C). We also tested the newly developed multiperiscopic peripheral prisms[14] that provide 100Δ (45° image shift) using a cascade of half-penta prisms (Fig. 3F). Because the lens blank holder is designed to enable tilting the lens blank in 5° steps to demonstrate the effect of tilts such as pantoscopic tilt and face-form on the retinal image, we specifically tested the effect of the pantoscopic tilt on the obscuration scotoma of the multiperiscopic prisms (Fig. 3F). We used the portrait orientation of the camera to reach a high-enough vertical field of view that included both upper and lower peripheral prism segments. To illustrate the effect of different back vertex distances, the lens holder could be moved closer or farther out from the reference point of the lens.

Fig. 4 shows the 3D-printed holder for a spectacles frame to directly fit spectacles-mounted low vision devices for the photographic depiction. The spectacles frame holder includes parameters such as pantoscopic tilt and face-form tilt and allows adjustment of the interpupillary distance (i.e., lateral shift of the spectacles frame), as well as vertical adjustment of the spectacles lens in front of the camera lens. The spectacles holder was used to photographically depict the field of view with conventional 57Δ (30° image shift) Fresnel peripheral prisms (Chadwick Optical, Harleysville, PA) in horizontal (Figs. 4A, B) and oblique configurations (Fig. 4C).[13,47] The interprism separation between upper and lower peripheral prisms was 10 mm.

Camera Settings

Camera settings (i.e., aperture size, exposure, focus, and dynamic range) were selected to cover a reasonable range of human eye characteristics and to illustrate their effects on the field of view. Because the effective focal length of the human eye and the camera lens we used are similar, we could simply select within a similar range of *F* numbers (f/2.8 to f/8) to simulate the pupil sizes of the human eye in the photographic depiction. We set *F* numbers of f/2.8, f/4, f/5.6, and f/8 to represent the human pupil size for dilated eye, mesopic, photopic indoor, and photopic outdoor conditions, respectively.[48,49] We also took photographs with the highest *F* number (f/22) to simulate a pinhole camera demonstrating the clear boundary and field size usually obtained with ray-tracing simulations.

To manually control the pupil size (i.e., *F* number), the exposure was automatically controlled by the aperture priority mode of the camera with compensated shutter speed. We used the center focus

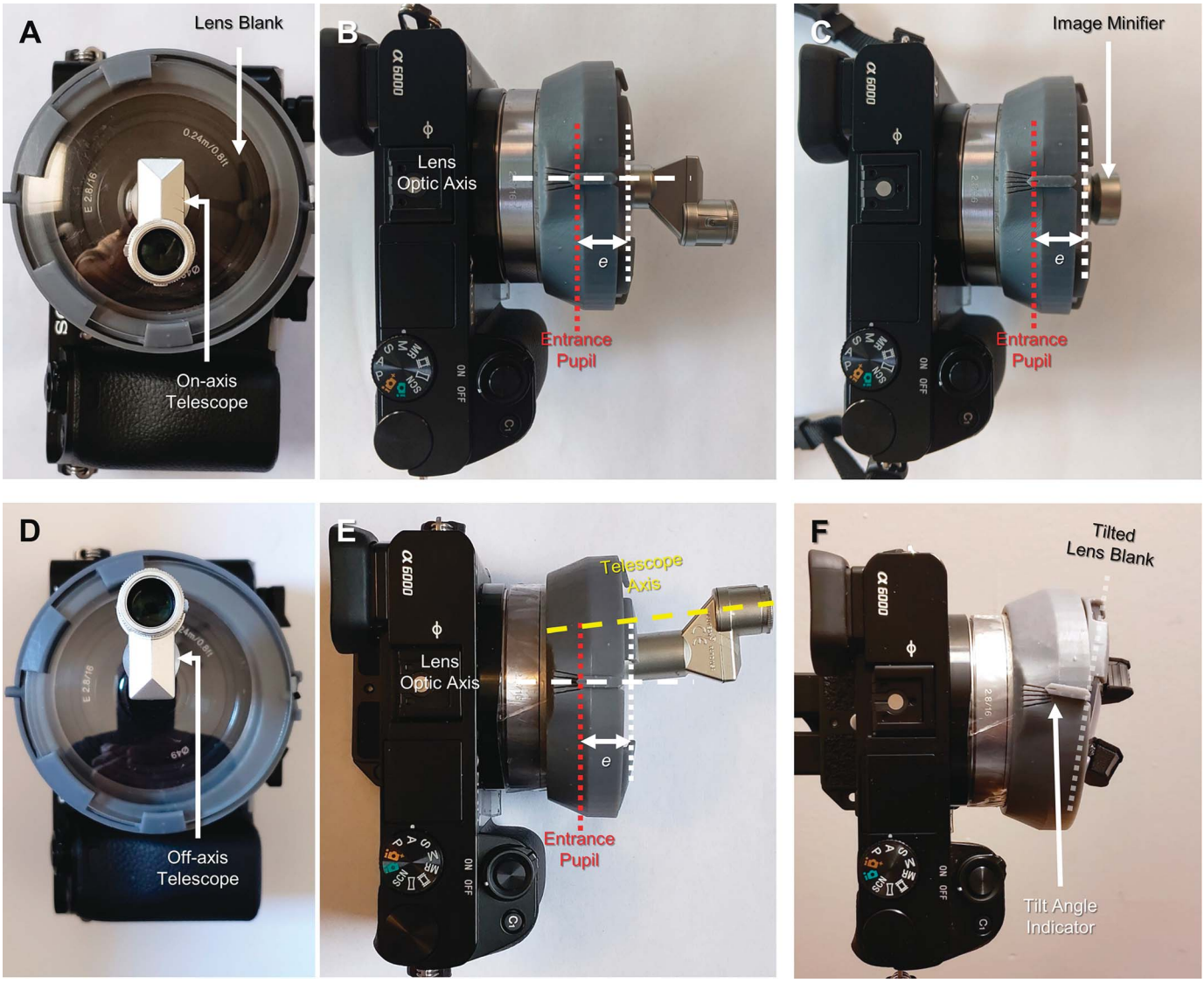

FIGURE 3. A 3D-printed holder for an ophthalmic lens blank. The holder mounts a 70-mm lens blank at a 17-mm reference-to-lens distance (*e*). Setup for the on-axis bioptic telescope at the front view (A) and the side view (B) and the on-axis image minifier (C; reverse telescope). Setup for the off-axis bioptic telescope at the front view (D) and the side view (E) and the peripheral multiperiscopic prisms (F) with 10° pantoscopic tilt. The lens blank holder can adjust the pantoscopic tilt in 5° steps.

(automatic focus through the center of the camera lens) and the center weight metering (automatic exposure control based on the brightness in the central field) to maintain similar brightness at the center of images across conditions. We turned on the high dynamic range mode of the camera to show as much field of view effect as possible. Note that we were studying the field of view and not the difference in the image quality across the devices or settings, although some of these differences are apparent.

RESULTS

To illustrate the field of view effects of the low vision devices as the retinal image, photographs were obtained in various practical scenarios (i.e., walking and driving conditions under different light levels). These results were compared with the perimetry diagrams with the same devices.

Keplerian Bioptic Telescope

We performed Goldmann perimetry (V4e target) with a normally sighted subject with and without a spectacles-mounted Keplerian bioptic telescope (Figs. 5A, B). The field of view through the telescope at the center (red solid outline) is surrounded by the ring scotoma (yellow solid outline), but the optical and obscuration scotomas are not distinguishable here.

The retinal image with the same bioptic telescope was depicted. For the indoor scenario, a conference poster attached to a corridor wall (7 m away) was used (Fig. 5C). The camera was mounted on a tripod at an adult eye level (1.6 m). The larger apparent size of the smaller field of view through the telescope represents magnification. The magnification power, the ratio of the field of view and its angular size of the

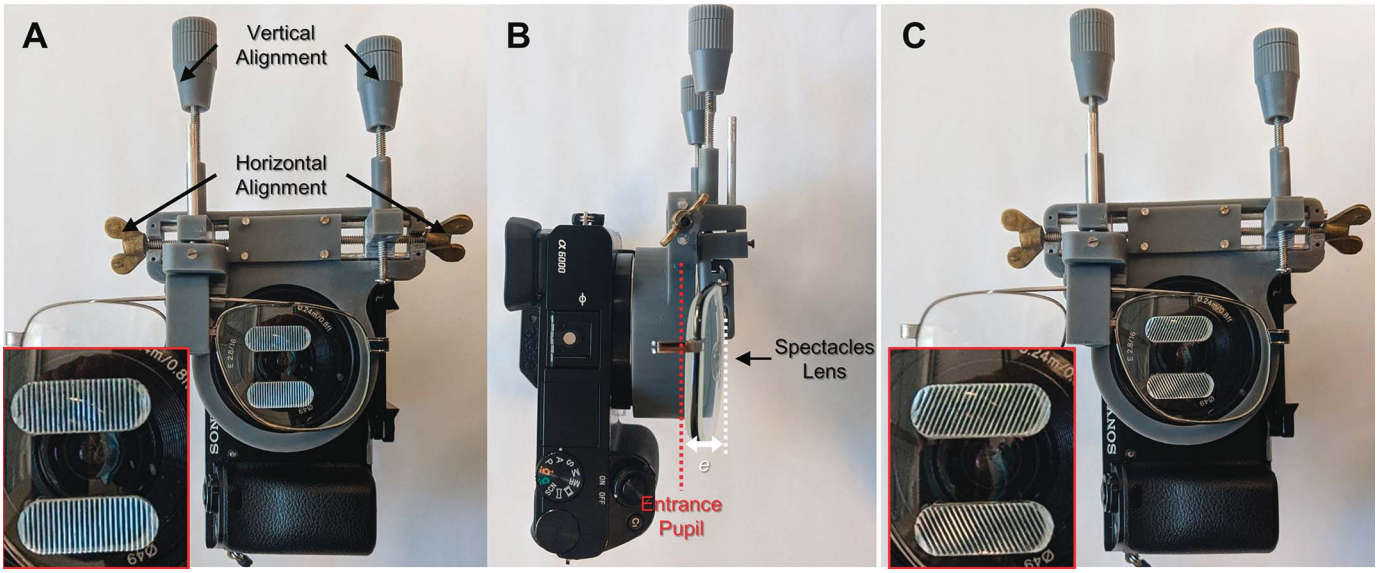

FIGURE 4. A 3D-printed spectacles holder that keeps the spectacles lens 17 mm (*e*) from the camera entrance pupil. The frame's brow bar and bridge position can be adjusted to align the optical centers of the spectacles' lens and the camera lens. Front view (A) and side view (B) of horizontal peripheral prisms (57Δ) glasses mounted on the camera and oblique peripheral prism configuration (C). Enlarged prisms are shown in the insets.

retinal image (e.g., the length of the red arrows in Figs. 5C, D), was constant across all pupil sizes calculated by using equation B2 in Appendix B, available at http://links.lww.com/OPX/A534. The retinal image captured by the photographic depiction clearly illustrates the difference between the optical and obscuration ring scotomas. The optical ring scotoma due to the magnification of the retinal image is invisible and only noticeable with careful tracking of missing objects between the fields of view in and outside the telescope (e.g., posters on the left and right walls close to the door). The obscuration ring scotoma is indeed photographed as a dark (narrower) ring. The optical ring scotoma (from the magnification) is a trade-off of the magnification for the field of view of the telescope (3× wider angular size of the retinal image); however, this additional obscuration ring scotoma is a waste of field of view and should be minimized. The photographic depiction also shows that the field through the telescope is cut as parts of obscuration scotomas caused by the erecting prism[50] in the Keplerian telescope.

Figs. 5D to H show the retinal images with the on-axis telescope captured with varying pupil sizes (*F* numbers). The larger pupil (smaller *F* number) results in larger retinal image through the telescope (thus a wider field of view through the telescope) with a narrower obscuration ring scotoma. In the largest pupil, the magnified view through the telescope and the view outside of the telescope are almost abutting at the boundary of the telescope, and the obscuration ring scotoma is narrowest and faint (Fig. 5D). With the smaller pupil sizes, the angular size of the retinal image through the telescope (and thus the field of view) is reduced with the enlarging obscuration ring scotoma. The result with f/22 (Fig. 5H), simulation of pinhole camera, illustrates the narrowest retinal image through the telescope (i.e., field of view) and the widest obscuration scotoma.

Fig. 6 illustrates the field of view effects with the 3× bioptic telescope in driving. At the eye position of a 175-cm-tall driver sitting in a car (Honda Crosstour, Tokyo, Japan), the camera was located 134 cm from the ground outside the car and 62 cm back from the vertical center of the windshield and aimed straight ahead. The retinal image through the on-axis telescope covers most of the windshield on the driver side. The optical ring scotoma of the narrow field of view through the telescope blocks most of the driving lane view through the windshield (Fig. 6B). The obscuration ring scotoma is visible with the smaller photopic pupil (f/8) owing to the bright outdoors. However, it falls outside of the windshield and thus does not restrict much of the driver's view, except on the right side of the windshield. Fig. 6C shows the photographic depiction results of the off-axis bioptic telescope (when not in use). Most of the driving time, the telescope is in this position, and the photographic depiction shows that the telescope and any ring scotoma do not interfere with the view through the windshield. Because of the position of the telescope, a small obscuration scotoma caused by the telescope body slightly interferes with the windshield view.

Image Minifier (Reverse Telescope)

A normally sighted observer's visual field (Fig. 7A) is wider than the field of view of the expander (about 50°), which results in the diplopia (Fig. 7B). Diplopia was purposely pursued in the perimetry by asking the subject to report two targets. A standard perimetric procedure would only show an enlarged physiological blind spot (compare the size in Figs. 7A, B). The image minifier is designed for patients who have narrower visual fields than the minifier's field of view, so the diplopia seen here would not affect these patients.

Photographic depiction, in the same corridor used previously for the telescope, illustrates field of view effects including diplopia and scotomas with the minifier as a retinal image. The field diagram is annotated over the photographic depiction of the corridor (Fig. 7C). The red and yellow solid lines illustrate the retinal image through the minifier and the field of view through the minifier with the indoor photopic pupil (f/5.6), respectively. The minification power, ratio of the angular size of the retinal image and the field of view of the expander (e.g., the ratio of the lengths of the red arrows in Figs. 7C, D), was constant across all pupil sizes calculated

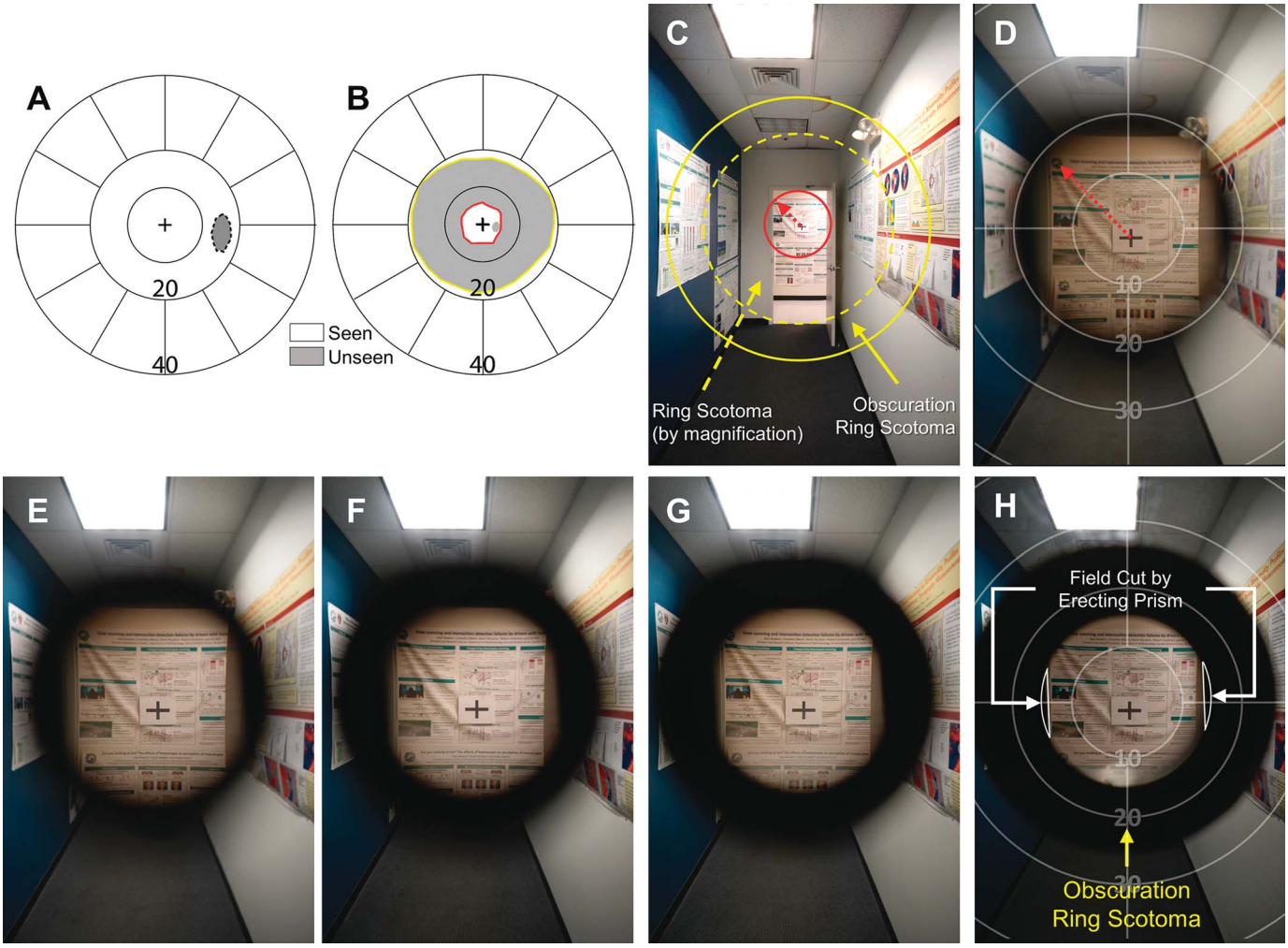

FIGURE 5. Field of view effects of a 3× bioptic telescope. (A) Field diagrams of a normally sighted right eye without telescope, showing only the optic nerve head scotoma, and (B) with the on-axis telescope. The field diagram illustrates the ring scotoma (gray area between red and yellow outlines) but does not distinguish between the optical (magnification) and obscuration ring scotomas. (C) A photograph of a corridor without the telescope. The red and yellow solid circles annotate the field of view seen through the telescope and the ring scotoma in panel B, respectively. The dashed yellow circle marks the retinal image boundary (optical ring scotoma) based on the indoor photopic pupil size (f/5.6) as shown in panel F. Photographic depiction of the corridor view with the telescope applying different *F* number settings: (D) f/2.8, (E) f/4, (F) f/5.6, and (G) f/8. Larger pupil (smaller *F* number) provides wider field of view and narrower obscuration scotoma caused by vignetting of the telescope aperture (e.g., the appearance of the logo in the left top corner of the poster with the smaller pupil). The size ratio between the red arrows in panels C and D illustrates the magnification power. (H) Photographic depiction with f/22. Note the obscuration scotomas from the erecting prism in the telescope, highlighted in panel H but visible in all other photographs.

by using equation B2 in Appendix B, available at http://links.lww.com/OPX/A534.

Figs. 7D to H illustrate the apparent minified image and diplopia, as shown on the retinal images. The obscuration ring scotoma created by the minifier body is seen in Figs. 7D to H. A normally sighted subject might see the obscuration ring scotoma during the perimetry. However, no missing field is recorded associated with that "scotoma" in the perimetry, as the field portions "blocked" by the obscuration scotoma are seen inside the field of view of the minifier. Importantly, both the diplopia and obscuration ring scotoma will not affect a potential user who has a residual central field narrower than the field of view of the minifier. The photographic depiction also illustrates the consistency of the perspective (compare ceiling tiles and poster lines across the retinal image) within and outside the image minifier.

Photographic Depiction of Peripheral Prisms in Walking

Because the peripheral prism was designed to detect colliding pedestrians approaching from the blind side of a patient with homonymous hemianopia,[13,51] we staged collision scenarios with a pedestrian in an open environment[44,52] to illustrate the field of view effects in the retinal image captured by the photographic depiction.

The 57Δ (≈ 30°) peripheral prism glasses were mounted on the camera at 1.5 m height in a wide-open room with a 1.9-m-high pedestrian, 2 m away, at bearing angles of 15 (Fig. 8A) and 30° (Fig. 8B). The camera was aimed straight ahead and focused on a far fixation target. The monocular field diagram (Fig. 1A) shows that the upper and lower 30° × 20° wide prism segments in the blind field are visible with the peripheral prisms

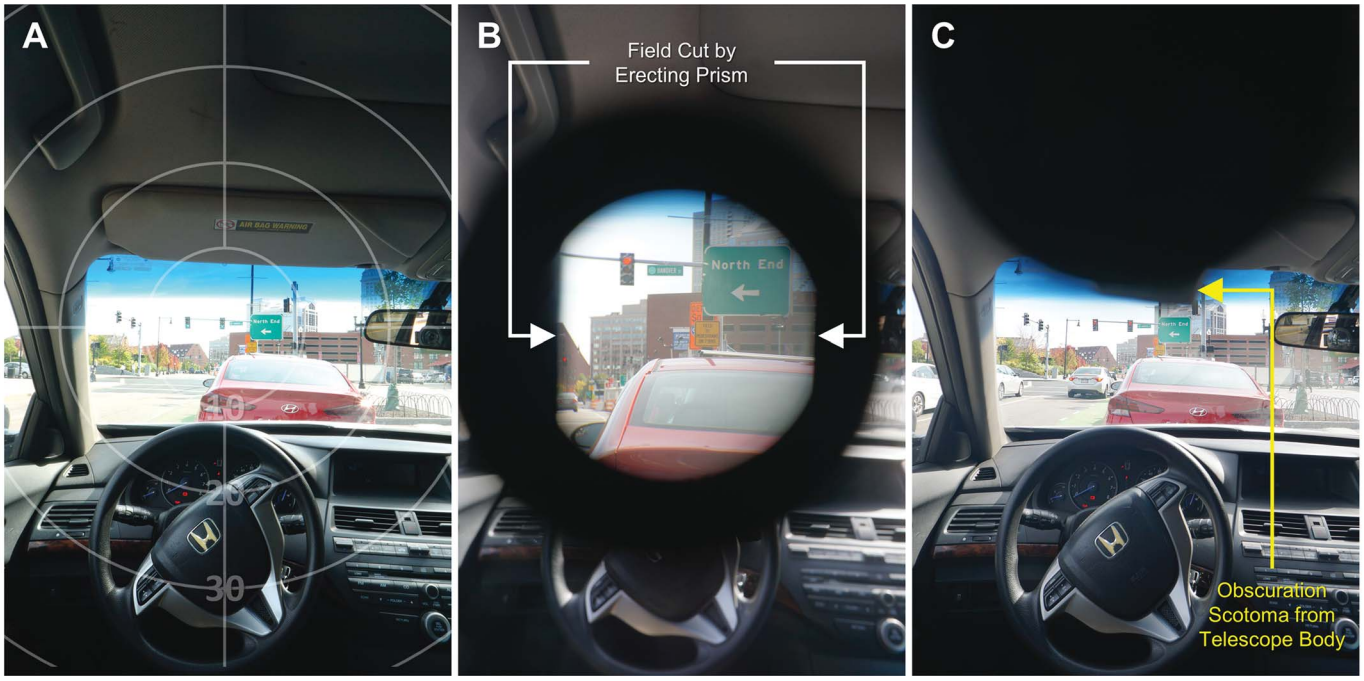

FIGURE 6. Photographic depiction with a 3× bioptic telescope in a car. (A) The forward driving scene without the telescope. (B) On-axis telescope (in-use position) with the photopic outdoor pupil (f/8). The retinal image through the telescope blocks most of the windshield forward view (optical ring scotoma). The obscuration ring scotoma is out of the windshield above and below and impedes vision only to the right (to the left, it is largely overlapping the A-pillar). Note the obscuration scotomas (more on the left) due to the erecting prism in panel B, which slightly restricts the horizontal field of view. (C) Off-axis telescope (when not in use), the retinal image through the telescope does not provide any view and also does not interfere with the view through the windshield. Note the obscuration scotoma caused by the telescope body slightly blocks the upper view through the windshield.

but does not illustrate where the retinal image is visible in the field and how the apical scotoma is seen.

Figs. 8C to F and D to J show the photographic depiction of the peripheral prisms, with pedestrians approaching on a collision course at bearing angles of 15 and 30°, respectively. The photographic depiction shows the retinal image through the prisms, which shows 30° shifted field of view. The pedestrian at 15° bearing/eccentricity on the blind side is shifted by 30° appearing at 15° eccentricity on the seeing side (Figs. 8C to F). The other pedestrian at the 30° bearing angle on the blind side is visible at the vertical midline on the retinal image through the peripheral prisms (Figs. 8G to J). The photographic depiction illustrates the invisibility of the apical scotoma (i.e., the scene behind the peripheral prism is blocked and replaced by the shifted view).

Various secondary field of view effects, not illustrated with the field diagram, are also visible in the photographs. Distortions of the shifted view[23,29,30] are illustrated by bent lines. The minified shifted view on the retinal image through the peripheral prisms results from the gradually increased effective prism power at higher angles of incidence.[23] Total internal reflection is visible as an arching boundary of a hazed area in the peripheral prisms on the blind side. Multiple horizontally overlapped ceiling lights (there is only one row of the square ceiling lights in the room) represent spurious reflections.[23] Different amounts of the visible scattering from multiple bases of Fresnel prism[23] in different pupil sizes are also illustrated. Note that any effects seen in the blind side of the photographic depiction become visible only when the patient scans with eye movements (but not with head movements) into the blind side.

The upper and lower peripheral prisms were computed to be 16° above and below the horizontal midline using the photographic depictions with the pinhole camera (Figs. 8F, J) by equation B2 in Appendix B, available at http://links.lww.com/OPX/A534, which matches the calculated field diagram with 10-mm interprism separation ($16 \approx \tan^{-1}(5/17)$). With the pinhole camera, the strips of multiple prism apertures (spaced by prism bases) in Fresnel prisms are visible. However, with consideration of the human pupil size (*F* number settings), the multiplexing effect enlarges the vertical field of view, reduces the interprism separation, and smooths multiple prism apertures in the Fresnel peripheral prisms (stronger effect in the wider pupil size cases). Because the upper prism was located 16° above the horizontal midline, the pedestrian was not detected through the upper prism when looking straight (see Discussion).

A dynamic video depiction was recorded to demonstrate these effects in mobility (see Video 1, available at http://links.lww.com/OPX/A535, and Video 2, available at http://links.lww.com/OPX/A536). The camera was moving forward on a cart to simulate walking, and the colliding pedestrian was approaching from the blind side on a collision course. The colliding pedestrian appears as a static (fixed bearing angle) looming pedestrian while the background is moving to create optic flow. Because the axes of the field of view and the retinal image through the prism are displaced horizontally, the optical flow of the shifted view in the peripheral prisms is inconsistent with the view outside the peripheral prisms (see Discussion).

Fig. 9 shows the calculated field diagram and photographic depiction carried out with the oblique peripheral prisms in the same scenarios. In the oblique configuration, the lateral prism power is reduced (from 30 to 27°) traded for the vertical prism power (13°) needed to reduce the gap between the upper and lower prism shifted views. The calculated field diagram shows that the blind field slightly above and below the horizontal midline is visible.

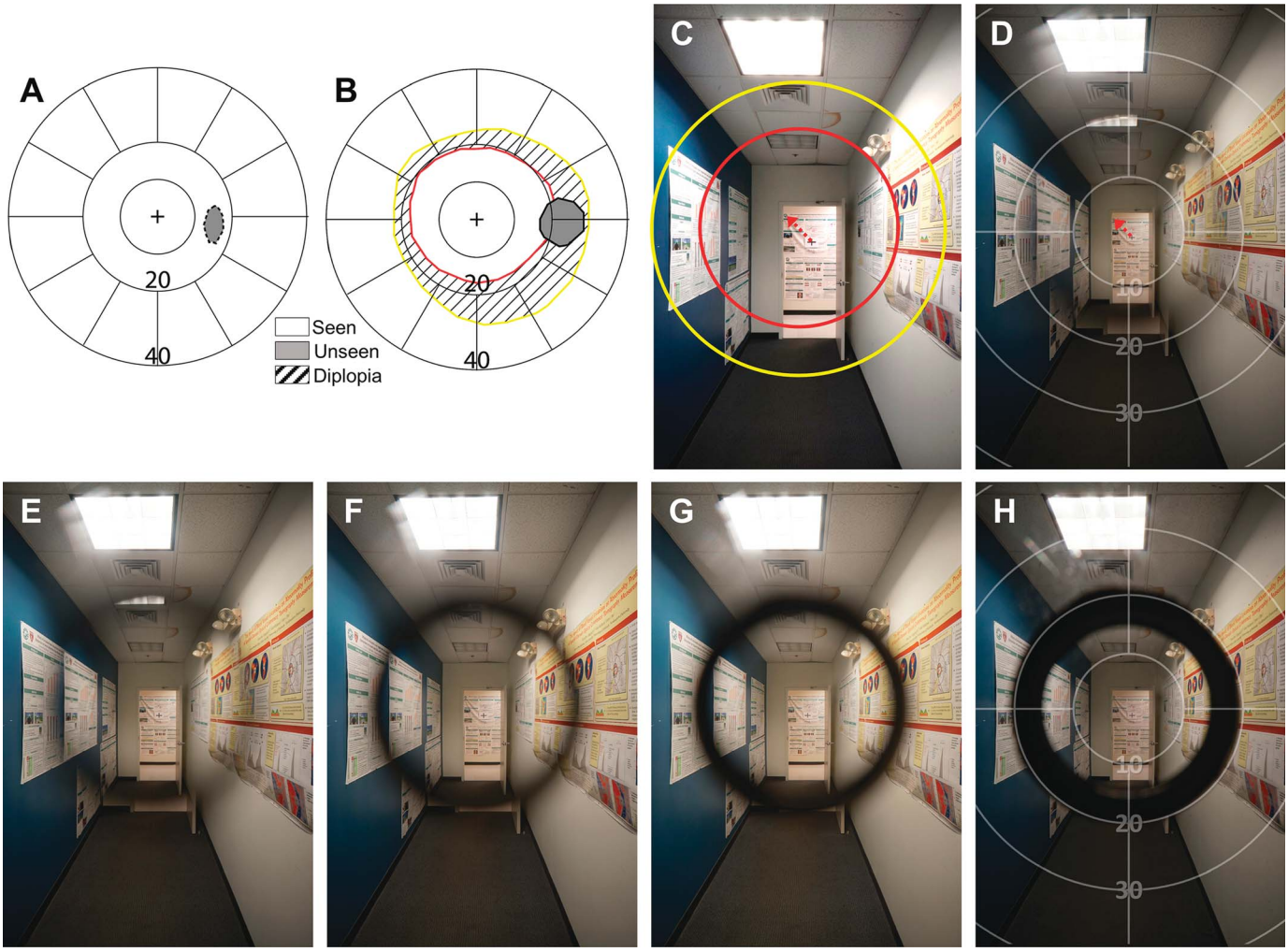

FIGURE 7. Photographic depiction of the field of view effects of 0.6× image minifier. Field diagram (Goldmann, V4e) of a normally sighted right eye without (A) and with (B) the minifier. The minification effect can be directly appreciated by the increased size of the optic nerve head scotoma and indirectly by the diplopia measured perimetrically. (C) A photograph of the corridor without the image minifier. The red and yellow circles annotate the retinal image through the image minifier and the field of view seen through it, respectively, with indoor photopic pupil (f/5.6). Photographic depictions with the minifier applying different *F* numbers: f/2.8 (D), f/3.5 (E), f/5.6 (F), and f/8 (G) cover the range of the human eye and f/22 (H) for the pinhole camera. The diplopia appears owing to the field of view being wider than the angular size of the retinal image through the image minifier. Although larger aperture shows wider retinal image (and field of view) with narrower obscuration ring scotoma, both effects are inconsequential because potential users' visual field is too narrow to see them. The ratio of red arrow lengths in panels C and D illustrates the minification power.

Whereas the shifted fields and the apical scotoma are visible at different vertical locations in the field diagram (Fig. 9A), the photographic depiction illustrates the shifted view on the location of the peripheral prisms images on the retinal image (see the same location of the peripheral prisms but the different shifted views in the prisms in Figs. 8 and 9), yet the apical scotomas are invisible.

The oblique peripheral prisms enable users to see the pedestrians in both the upper and lower prisms while looking straight at the fixation target. Because of the reduced horizontal prism power, the 15° pedestrian (appearing more centrally in Figs. 9B to E than Figs. 8C to F) and the 30° pedestrian are shifted by a smaller angle into the seeing field (only a stretched right leg is visible in Figs. 9F to I). The gap between the upper and lower shifted views was not completely closed, as the shoulder and neck were not visible in the shifted view (about 8° gap remaining in Fig. 9A). Considering the multiplexing effect with wider human pupil sizes, the gap between the upper and lower shifted views was further closed, which is specifically helpful to use the upper oblique prisms (i.e., more of the pedestrian's head is visible in upper prisms with larger pupil). The dynamic video depiction was recorded also with oblique prisms (Video 3, available at http://links.lww.com/OPX/A537, and Video 4, available at http://links.lww.com/OPX/A538). While walking with oblique peripheral prisms, because of both horizontal and vertical shifted views through the oblique prism, the optical flow seen within the oblique peripheral prisms and outside the prisms differs in both horizontal and vertical directions.

Photographic Depiction of Peripheral Prisms in Driving

The effects of peripheral prisms in driving (Fig. 10) were depicted using the same camera settings as used with the telescope. A colliding pedestrian was approaching from the blind side at 10° bearing angle 12 m away. The horizontal peripheral prisms in the car provided no usable field expansion because they only affected views above and below the windshield (Fig. 10B). The oblique peripheral prisms shifted

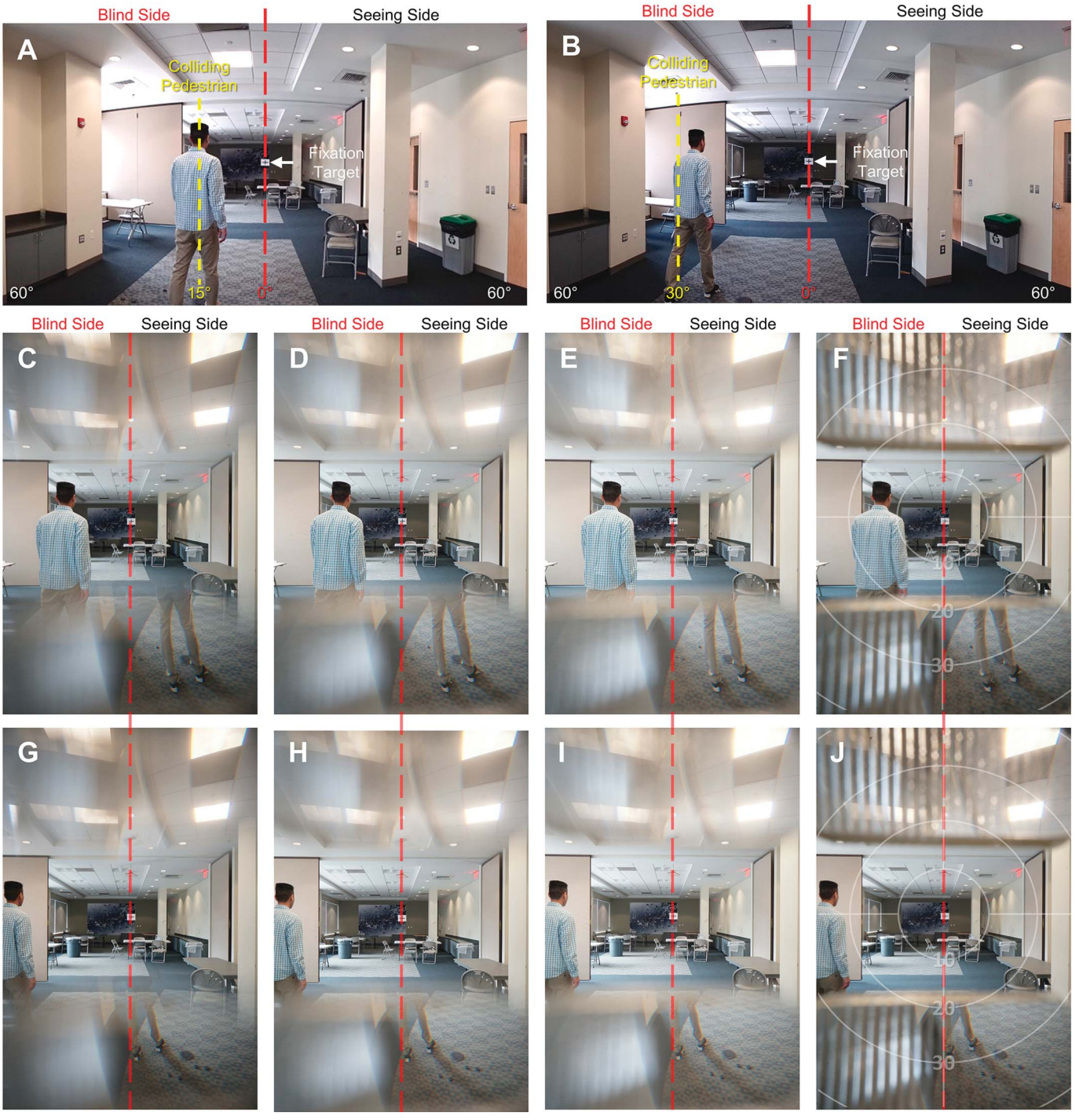

FIGURE 8. Photographic depiction with 57Δ Fresnel horizontal peripheral prisms for left homonymous hemianopia (only left lens). Panoramic images of the walking scenario with colliding pedestrians approaching at bearing angles of 15 (A) and 30° (B). The effect of horizontal peripheral prisms with pedestrians at bearing angles of 15° (C to F) and 30° (G to J) shows the shifted view and the apical scotoma (not visible but notable as missing legs of the folding chair on the right side). *F* numbers were varied from f/2.8 (C, G) to f/5.6 (D, H), and f/8 (E, I) covering the range of the human eye's pupil, and f/22 (F, J) representing the view with a pinhole camera. Details are shown here and not available in the field diagram, including the stronger minification close to the total internal reflection boundary (see the thinner legs of the 30° pedestrian in the shifted view), the limited eye scanning range due to the total internal reflection (the boundary with the hazed area at about 5° into the blind side), the total internal reflection and spurious reflections (multiple lateral mirror images of the ceiling lights, in the upper prism segment), multiplexing effects at the prisms' horizontal boundaries (superimposed shifted and normal views) and multiple prism apertures (smoothed from pinhole results in F, J), and varying levels of scattering from the bases of Fresnel prism (less visible scattering in narrower pupil). The effects on the blind side are only visible when the patient scans into the blind side with the eye. The upper horizontal prism does not capture colliding pedestrians.

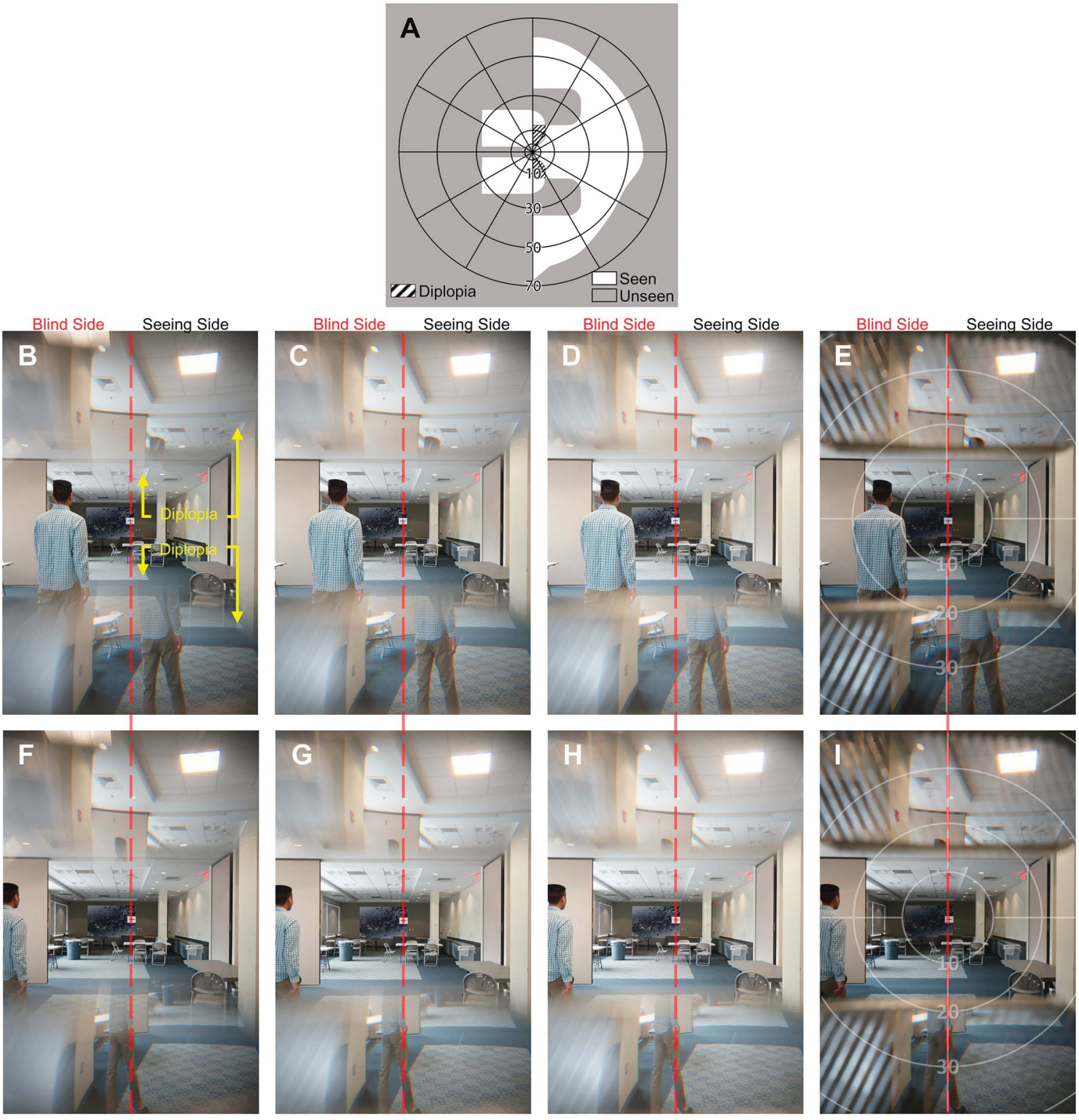

FIGURE 9. Photographic depiction of the effect of 57Δ oblique peripheral prisms (25° oblique tilt) for left homonymous hemianopia (left lens only). (A) Calculated field diagram using a pinhole camera model. Lateral 27° wide segments of the blind field above and below the horizontal midline are made visible. Small diplopia occurs around the apex of the oblique peripheral prisms. Photographic depiction of the oblique peripheral prism effects with 15 (B to E) and 30° (F to I) pedestrians (illustrated in Figs. 8A and B, respectively) is demonstrating both laterally and vertically shifted views and actual rendition of the apical scotoma (invisibility of the folding chair legs in the right side). Small diplopic areas are illustrated twice in both inside and outside of the oblique prisms. Both the upper and lower oblique prisms image the 15° pedestrian when the camera is aimed straight ahead. However, because of the reduced lateral prism power, only part of the right leg of the 30° pedestrian is seen in the lower segment. *F* number was varied from f/2.8 (B, F), f/5.6 (C, G), and f/8 (D, H) covering the range of the human eye and f/22 (E, I) for the pinhole camera. The gap between the upper and lower prisms is affected by the pupil size. Note the more visible shoulders and neck of the pedestrian in the leftmost column (f/2.8) than the third column (f/8).

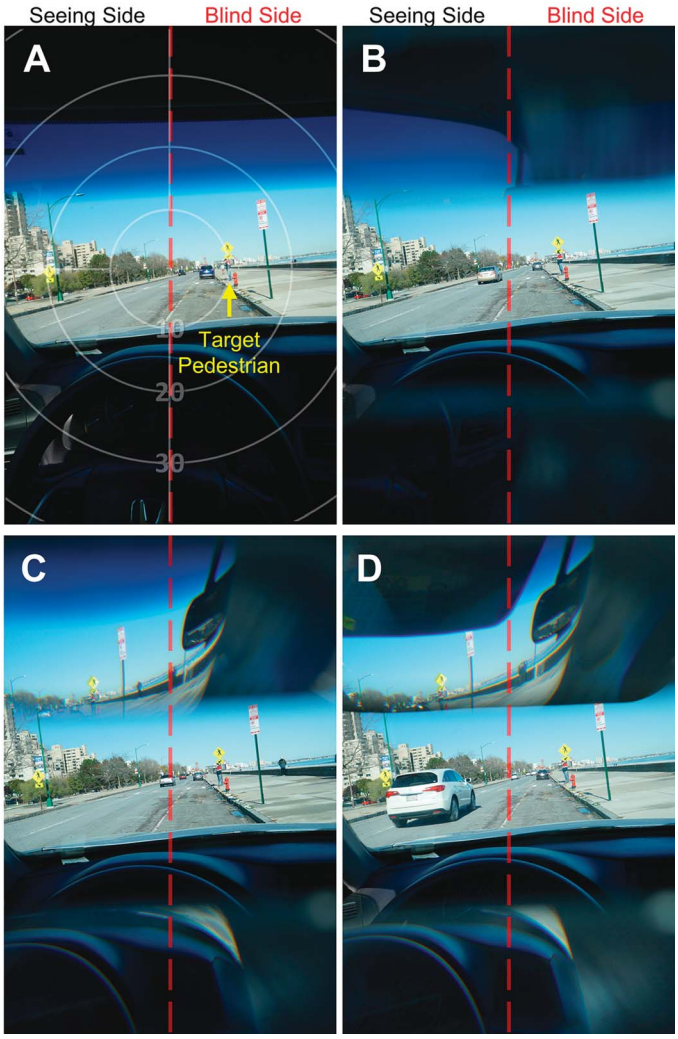

FIGURE 10. Photographic depiction of 57Δ peripheral prisms for right homonymous hemianopia (photopic outdoor pupil, f/8). (A) Driving scenario with a pedestrian at 10° bearing and 12 m away. (B) The same scene through horizontal peripheral prisms. Neither upper nor lower prism shows any useful field of view for the driving. (C) With oblique peripheral prisms. The lower peripheral prism is still not useful. The upper peripheral prism shifts the pedestrian from the blind side to the seeing side, but the image contrast near the pedestrian location is low. D, The oblique peripheral prisms with the sun visor pulled partially down. The visor improves the contrast of the shifted view.

the views from within the windshield, as designed, and thus made the blind-side pedestrian visible. Even with the smaller pupil in this bright photopic outdoor condition (f/8), the central boundary of the peripheral prisms is blurred, and the pedestrian has lower contrast.

Adjusting the sun visor down to block the bright light at the boundary of the prism increased the contrast of the shifted view at the horizontal boundary, rendering the pedestrian more visible. Although the extended visor on the right partially blocked the upper unshifted view, it is blocked on the blind side of the driver. The lower peripheral prism in both horizontal and oblique configurations was not found to be helpful, an effect that could not be determined from the field diagram. In both cases, it did not cover the view through the windshield.

Multiperiscopic Prism

The multiperiscopic prism is a recently developed high-power image shifting device using reflective half-penta prisms, which provides 100Δ (≈ 45°) power with minimal distortion.[14] To minimize the obscuration scotoma from the protrusion structure, the multiperiscopic prism is mounted with a tilt to match the line of sight (Fig. 11A). However, the spectacles' pantoscopic tilt may change this angle and, as a result, increases the obscuration scotoma.[14] We used photographic depiction to demonstrate the field of view effect (prism shift) and evaluate the effect of pantoscopic tilt on the obscuration scotoma by rotating the lens blank on the 3D-printed holder.

The photographic depiction illustrated 45° high power of multiperiscopic prism (Fig. 11). Comparing with conventional Fresnel prisms (Fig. 8), much less distortion and higher contrast were demonstrated in the photographic depiction. The undistorted shifted view clearly illustrates the viewpoint rotation (45° axis rotation between the axes of the retinal image and the field of view through the multiperiscopic prism). With additional pantoscopic tilt (Figs. 11D, E), the prisms are tilted down and additional obscuration scotomas appear, resulting in a reduction of the vertical extent of the shifted field of view. The change of the obscuration scotoma at the central boundary of the prisms was minimal.

Effects of Back Vertex Distance

The effects of different back vertex distances were demonstrated with the telescope and the peripheral prisms. The back vertex distance was varied within a range of ±3 mm to evaluate the effects of individual variations. A closer bioptic telescope due to shorter back vertex distance (Fig. 12B) results in a wider retinal image through the telescope and thus a wider field of view through the telescope. At the same time, closer fitting results in larger optical (i.e., 3× of field of view) and obscuration ring scotomas. Farther telescope fitting

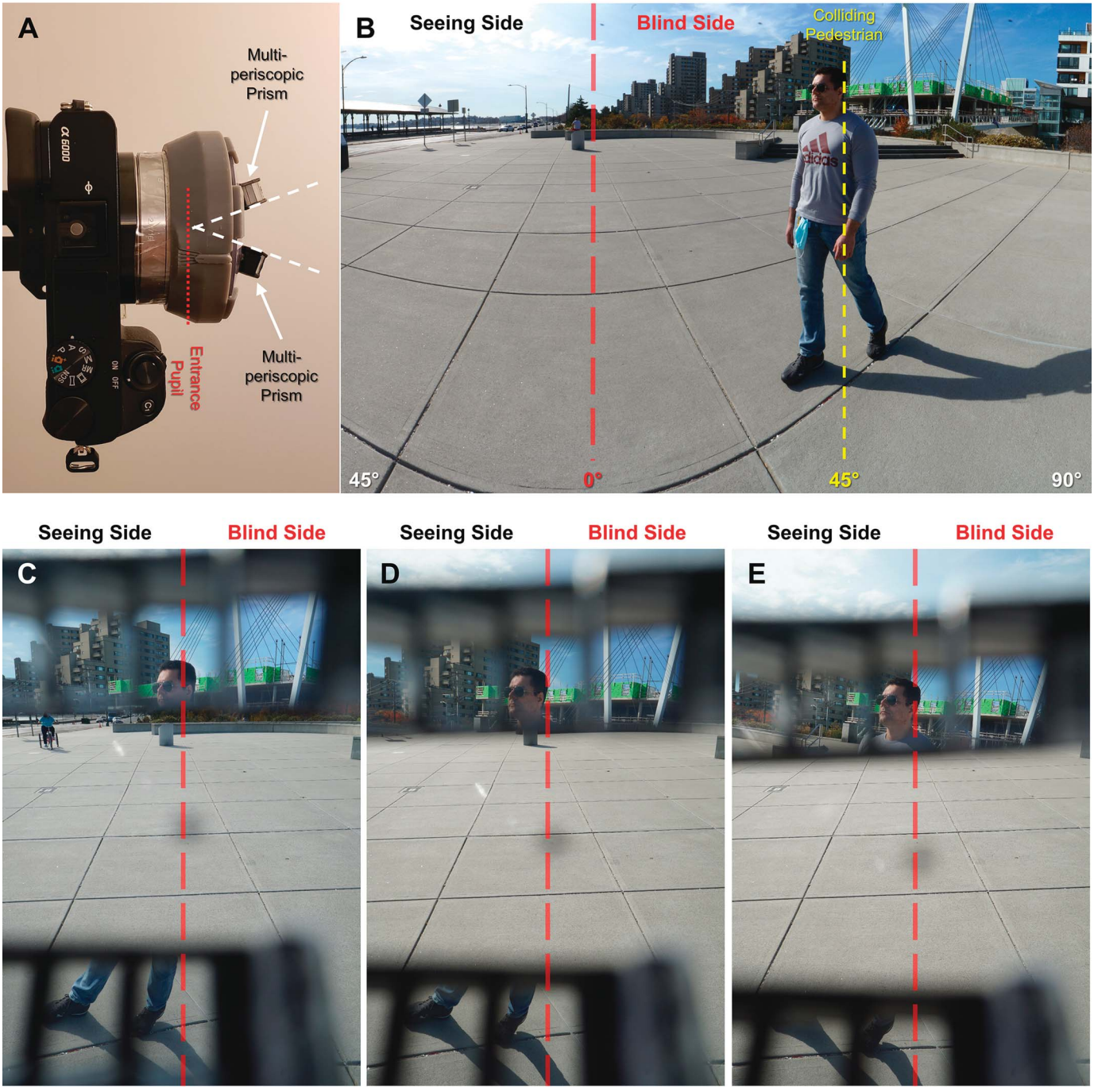

FIGURE 11. Photographic depiction of multiperiscopic prisms (f/8 for outdoor photopic condition). (A) Multiperiscopic prisms mounted with tilts to match the line of sight (white dashed lines). (B) Panoramic image of a walking scenario with colliding pedestrians at 45° bearing on the blind side. (C) Photographic depiction through the multiperiscopic prism shows a 45° shift with less distortion and higher contrast (compare with the Fresnel prism in Fig. 8). A viewpoint rotation rather than just an image shift is apparent in the perspective change of the cement tiles and lines near the pedestrian leg seen in the lower prism. Photographic depiction of the multiperiscopic prism with 5° (D) and 10° (E) pantoscopic tilts. A black spot is marked on the center of the lens blank to illustrate the effect of pantoscopic tilt or a head tilt down. With more pantoscopic tilt, the multiperiscopic prism aims at the pedestrian and the ground at a different angle, and thus, the viewpoints are changed (e.g., rotation of cement line). The obscuration scotomas grew slightly wider, but the change was minimal.

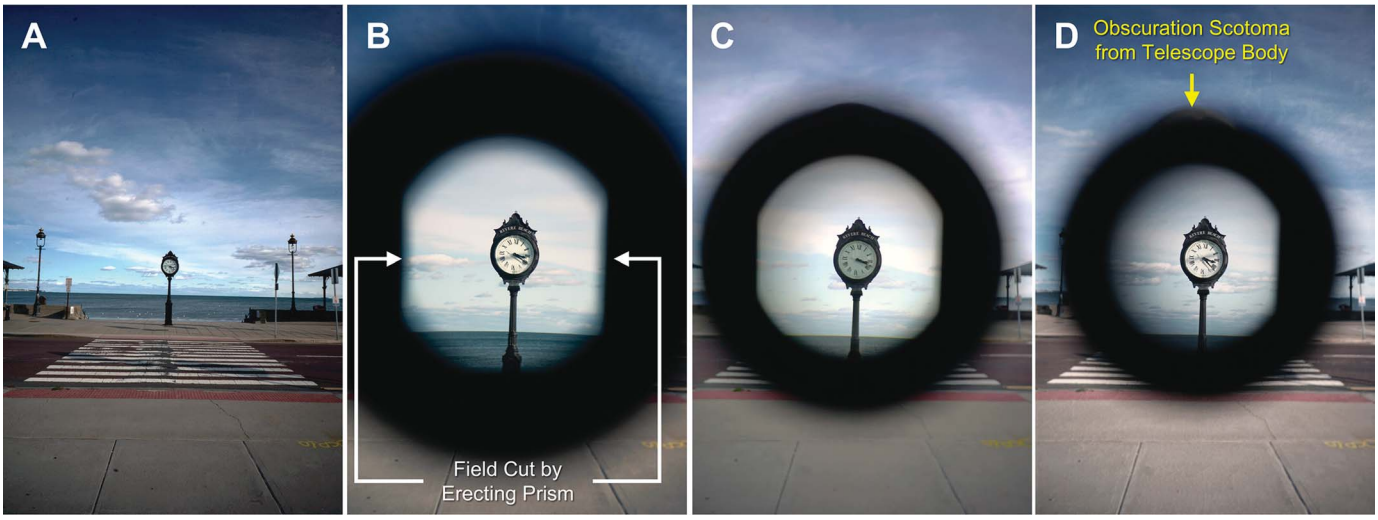

FIGURE 12. Effect of back vertex distance on the field of view with a 3× Keplerian bioptic telescope. (A) A street clock photograph (f/8 for photopic outdoor condition). The field of view on the retinal image with back vertex distance of 10 (B), 13 (C), and 16 mm (D). Telescope closer to the eye (B) provides a wider retinal image through the telescope (i.e., wider field of view) than farther telescope (D) but also with wider ring scotoma due to both wider optical and obscuration scotomas. Note the scotomas caused by the erecting prism in the telescope (straight vertical field cuts) and the small obscuration scotoma from the telescope body.

has smaller ring scotomas, but the field of view is also narrower (Fig. 12D). Regardless of the back vertex distance, the magnification power is unchanged. Note that the field cut by the erecting prism here further limits the field of view (see Discussion).

The effect of back vertex distance on the peripheral prisms is illustrated in Fig. 13. Because we used the spectacles-mounted peripheral prisms, only 3-mm farther back vertex distance (16 mm) than the normal 13 mm was tested. The longer back vertex distance reduced the angular gap between the prisms, which brought the shifted view through the windshield. Although the horizontal prisms were still not useful, the whole body of the pedestrian and the street closer than the pedestrian were visible in the upper and lower oblique prisms, respectively.

DISCUSSION

This article documented calibrated field of view effects of several low vision devices (bioptic telescope, image minifier, and a few types of peripheral prisms). We used a commercial camera and wide field of view lens to match the focal length and pupil size effects of the human eye. To demonstrate the possible use of photographic depiction, the field of view effects were recorded in practical scenarios (walking and driving with different pupil sizes) and considering practical fitting parameters (i.e., back vertex difference and pantoscopic tilt). The photographic depiction of the field of view effects we presented helps analyzing the functionality of these devices. It also revealed additional interesting field of view effects that are often missed in perimetry.

The impact of different pupil sizes on the view of obscuration scotoma from the packaging or body of the devices was illustrated as different amounts of vignetting (e.g., telescope, minifier, and multiperiscopic prisms).[14] With devices that have seamless boundaries (e.g., Fresnel peripheral prisms), varying pupil sizes resulted in different levels of multiplexing effect (superimposed views from both within and outside the devices) at the boundaries. These vignetting and multiplexing effects affect the users and thus affect the field extent through the devices measured in the perimetry. It may be one of the sources of the difference between the expected field extent from the ray-tracing calculation and the perimetry measurement.[21,34] Scattering at the multiple base structures of the Fresnel prism is also illustrated with different sizes of pupil. Even though there are always scatterings from each serration of Fresnel prism, which is smaller than human eye pupil, pinhole-like cameras such as conventional simulation or calculation cannot illustrate the scattering, and thus, it shows up as multiple strips of apertures.[33] The photographic depiction demonstrated how the pupil size affects the perception of all these pre-existing diffractions or scattering effects at the boundary of the devices.

With the bioptic telescope, a ring scotoma can be measured perimetrically and is largely a result of the magnification,[25,26] although it has been frequently blamed on obscuration by the telescope body in the literature.[53–57] This misinterpretation may be because the obscuration ring scotoma is easily noticeable when using the telescope (optical ring scotoma is invisible) and the perimetry results do not distinguish the optical and obscuration ring scotomas. The photographic depiction clearly distinguishes between the optical and obscuration ring scotomas and shows that usually only a small portion of the ring scotoma is attributable to the obscuration by the telescope aperture (Fig. 5). Although the ring scotoma of the monocular bioptic telescope can be compensated by the fellow eye under binocular viewing,[58] the ring scotoma does represent loss of field of view in bilateral bioptic telescopes fitting.

Our results called attention to the field cut by the erecting prism in the Keplerian telescope (Figs. 5, 7). This illustration of the field cut can guide the selection of telescope orientation for which, currently, there is no clear suggestion by the manufacturer.[46] Because a wider horizontal field of view is preferred,[38,59,60] orienting the telescope to bring these field cuts to the upper and lower field of view (i.e., orthogonal to the orientation shown in Fig. 3) may be beneficial. Small additional obscuration scotomas from the prism and objective lens package of the telescope, where the prism is

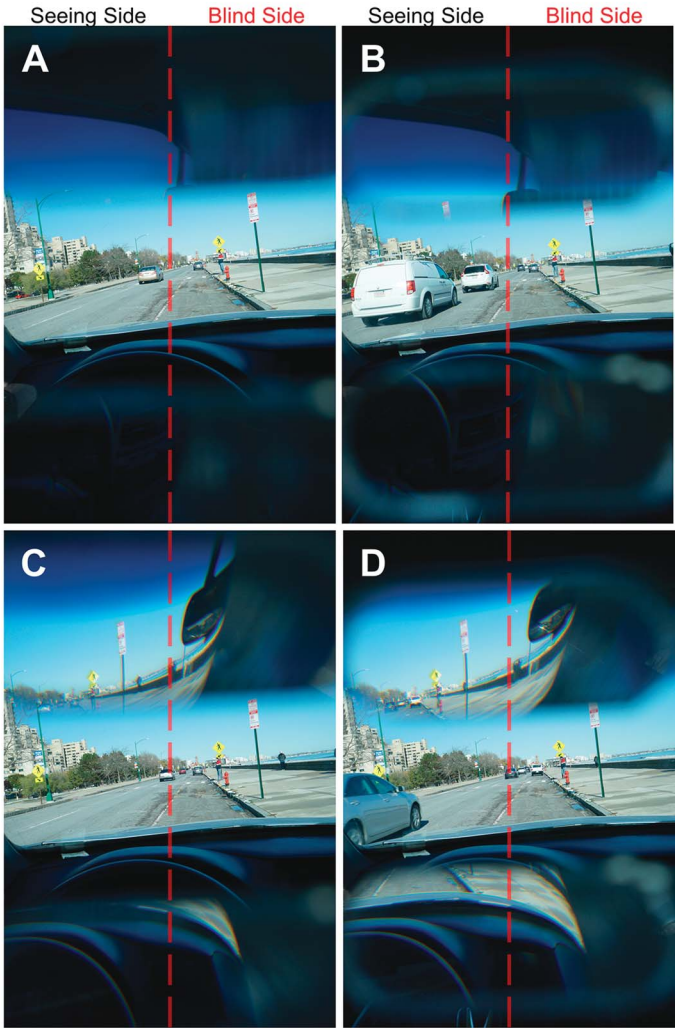

FIGURE 13. Effect of larger back vertex distance on peripheral prisms for right homonymous hemianopia (photopic outdoor pupil, f/8). Upper row: horizontal peripheral prisms with (A) 13-mm and (B) 16-mm back vertex distances. With longer back vertex distance, upper horizontal prism now shows a partial field of view through the windshield, but that field of view is not helpful for driving. Lower row: oblique peripheral prisms with (C) 13-mm and (D) 16-mm back vertex distances. With longer back vertex distance, upper oblique prism fully shows the pedestrian from the blind side, and lower oblique prism also shows the road pavement and the sidewalk seen through the windshield.

housed, are also visible (Figs. 6C, 12D) in the photographic depiction, which slightly affected the windshield view at the not-in-use position. The same preferred orientation of the telescope to move the internal field cut will also move this small outside obscuration scotoma to overlap the A-pillar of the car and stay out of the windshield view. The photographic depiction illustrates these details and thus helps us make these observations and recommendations for better fitting.

The photographic depiction may illustrate the difference in magnitude of eye and head scanning with the telescope. As shown in Figs. 5C, D with the red arrows, because of the 3× magnification, the eye scanning within the field of view of the 3× telescope (the length of the arrow in Fig. 5D) requires three times larger than head scanning without the telescope (the length of the arrow in Fig. 5C). This may explain the effective use of head scanning observed with the telescope. The head scanning with the telescope has been pointed as a limitation of the telescope use, as head scanning is slower than eye scanning.[61] However, the understanding supported by the depiction shows that this may not be the case. In fact, the angular size of the retinal image through most telescopes (>40°) is much wider than the size of most saccades (>15°).[62] For example (Fig. 5), to scan an approximately 10° field of view through the telescope, approximately 30° of excessive eye scanning is required on the magnified retinal image through the telescope. The same shift in the retinal image will be achieved with just 10° of head scanning. This also illustrates the vestibular-ocular reflex resulting from the increased motion, which accompanies head-mounted magnification.[63,64] This limitation may be one of the reasons that head scanning with the telescope is preferred.

A new finding with the peripheral prisms is the illustration of viewpoint rotation rather than that of the shift seen in the photographs. The field of view through the prisms is described and illustrated as a shifted view.[12,18,52] In fact, the prism view results in a shift in the angular domain, not a linear distance domain.[23] The shift in the angular domain means rotation of the viewpoint (i.e., rotation of the axis of the field of view from the axis of the retinal image by the angular prism power), which results in perspective difference

between the view through and outside of the prisms. This effect is difficult to observe in the conventional or Fresnel prism because of strong prism distortions (Figs. 8, 9),[23] but the photographic depiction through the mostly distortion-free multiperiscopic prism illustrates the rotation of viewpoint (i.e., the lines on the ground in Fig. 11). Because the shifted view principle is the same in both the multiperiscopic and conventional prisms, we should regard the shifted view in the conventional prism also as a rotation of the viewpoint with additional distortion.[23]

In walking, the photographic depiction demonstrated that the rotated viewpoint in the peripheral prism has noticeably different optical flows than outside the prism (see optical flows in Video 1, available at http://links.lww.com/OPX/A535, and Video 4, available at http://links.lww.com/OPX/A538, further affected by the prism distortion). This difference may cause binocular rivalry with the optical flow of the moving background in the fellow eye and thus may reduce detection performance in the peripheral prisms.[65–67] In driving, although the oblique peripheral prisms show optical flows in the shifted view through the windshield, the fellow eye sees a static scene of the car interior. Therefore, there may be no binocular rivalry because only the shifted view through the windshield provides the optical flow.

The photographic depiction also enabled examining the secondary field of view effects in Fresnel prisms (distortion, spurious reflection, and total internal reflection), which are not possible to illustrate in the field diagram (i.e., distortion). These issues mostly exist or are of larger magnitude in the blind side of homonymous hemianopia. However, with only a small (~5°) eye scanning into the blind side, these artifacts become visible. Interestingly, color dispersion[31,32] was barely noticeable in the photographic depiction of the Fresnel peripheral prisms. Because the Fresnel prism has a shorter optical path length than the conventional ophthalmic prism, no noticeable color dispersion may be understandable. However, the light scattering from the multiple base surfaces was illustrated in the photographic depiction with the effect of the pupil sizes, which may cause low contrast and other image quality limitation.[23,31,32,68]

The photographic depiction of the peripheral prisms also raises a question about their utility in pedestrian detection. When we assumed that a patient with homonymous hemianopia looks straightforward and keeps head straight while walking, the upper horizontal peripheral prisms did not show the colliding pedestrian (Fig. 8), whereas it did with the oblique peripheral prism (Fig. 9). However, if the head tilt angle[69] is considered during walking, the pedestrian may become detectable through upper horizontal prisms and the efficacy of the horizontal peripheral prism may be increased (Kurukuti NM, et al. IOVS 2020;61:ARVO E-Abstract 2771). Further analysis of the peripheral prisms' efficacy with consideration of head tilt and bobbing during walking will be required.

Questions regarding the efficacy of the lower peripheral prism segment in driving were also raised by the photographic depiction. We already knew that oblique peripheral prisms are needed for driving with homonymous hemianopia.[47,70,71] However, in our photographs, the lower oblique peripheral prisms did not display much useful information through the windshield (Fig. 10). Because individual parameters (driver seat height and distance, head tilt angle, back vertex distance, and the windshield size) and fitting parameters (interprism separation and oblique tilt angle) affect the vertical shift through the oblique prisms, further analysis to quantify the efficacy and possible configurations will be required. Thus, the current photographic depiction results alerted us to a number of design and fitting issues that were not obvious before, even if they should have been.

The multiplexing effect in different pupil sizes (i.e., lighting condition) on the peripheral prisms should also be considered in detection performance. Specifically, the photographic depiction illustrated how the pedestrian detected through the oblique peripheral prisms looks in the environment we simulated (looking straight during walking and driving), even though the part of the pedestrian visible through the prisms was small. This multiplexing effect could be reduced by lowering the sun visor to improve the contrast around the boundary of the upper prism's shifted view. The sun visor creates an obscuration scotoma for the fellow eye (not shown in Fig. 10), and thus, the apical scotoma is manifested in this situation (i.e., the obscuration scotoma and apical scotoma at the same location). Because the location of the scotoma is as high as the sun visor during normal use in driving, it may not further block useful driving information through the windshield.

The photographic depiction illustrates the retinal images with the devices, the image before being processed by the human visual system. Various visual characteristics such as reduced spatial resolution and contrast sensitivity with eccentricity are not illustrated. Pathological scotomas and even physiological blind spots are not illustrated with the photographic depiction. To better simulate the scene perceived through the devices by a user, additional image processing of the images obtained by the photographic depiction may be helpful (i.e., simulating the changes in resolution and contrast sensitivity with eccentricity).[72–74] Accurately simulating how patients with field loss perceive is not as simple as putting black patches to represent a scotoma.[75,76] Instead of applying any additional image processing, any normally sighted or low vision observers can experience the performance of the device from the image captured by the photographic depiction through their own visual system if it is displayed at the right angular size. Because the pictures of the photographic depiction in this article would be printed or displayed on a monitor, we expect the readers at the usual reading distance would observe them at a much smaller angular size than the correct angular size. If each photographic depiction result is observed in the correct angular size (73 $\times$ 52°) at high resolution (e.g., a 42-inch screen observed from 54 cm), observers can perceive visual effects owing to the effect of their visual system and low vision perception on top of the photographic depiction of the device. This may demonstrate the effect of the device being considered to the patients before the device is ordered.

The current photographic depiction is only presenting monocular effects. Functionality or utility of the low vision devices interacts with binocular vision, such as binocular visual confusion for field expansion with unilateral peripheral prisms, and elimination or reducing the effects of the ring scotoma in the telescope. One possible approach to presenting the binocular effect might be photographic depictions of left and right eye views that are shown on a stereoscopic display system such as a head-mounted display. A head-mounted display may be able to provide wider angular size and binocular-viewing requirements, although the resolution in current displays may not be sufficient yet to provide correct illustration centrally.

Optical simulation tools or 3D rendering software can generate similar illustrations from virtual rendering cameras. A virtual environment and rendering camera could easily generate virtual photographic depiction, but these are usually based on ray tracing with a pinhole camera model.[33] The retinal image through the low vision devices and the obscuration scotoma with the finite pupil of the human eye is different from the simulated pinhole result (f/22). Although the pupil size effect could be implemented with the incorporation of a human eye model in a professional optical simulation or

additional depth of field rendering in the rendering camera, the photographic depiction may still be beneficial owing to its simplicity and testability in real-world environments.

We prototyped the photographic depiction with a mirrorless camera and pancake lens to illustrate many possible optical effects in various environments. A conventional smartphone camera may be used for limited photographic depiction if there is a simple way to keep the back vertex distance of the spectacles-mounted low vision aid from the camera. Because most smartphone cameras have a fixed pupil size (*F* number), the photographic depiction with a smartphone camera may not be able to provide the effect from the pupil size changes (Appendix C, available at http://links.lww.com/OPX/A534).

Our photographic depiction illustrates the retinal image and field of view effects of the low vision devices but is not a replacement for the field diagram. For the size or magnitude of the field of view effects, the field diagram is beneficial in addition to the photographic depiction. In this article, we focused on introducing the photographic depiction technique and demonstrating what it can show in several scenarios. There may be other beneficial scenarios and low vision devices that we did not test here. Although we introduced the photographic depiction in the limited scenarios with a static field of view, the photographic depiction may also be applicable to the dynamic field of view such as eye scanning or head scanning with further development of the holder.

ARTICLE INFORMATION

Supplemental Digital Content: Appendix A, available at http://links.lww.com/OPX/A534: empirical method to determine the reference point of the perspective in the camera lens is described.

Appendix B, available at http://links.lww.com/OPX/A534: the equation describing the distance to angular-size conversion.

Appendix C, available at http://links.lww.com/OPX/A534: possible photographic depiction option with a smartphone camera.

Video 1, available at http://links.lww.com/OPX/A535: dynamic video depiction: simulated walking with a colliding pedestrian at 15° bearing angle with 57Δ Fresnel horizontal peripheral prisms.

Video 2, available at http://links.lww.com/OPX/A536: dynamic video depiction: simulated walking with a colliding pedestrian at 30° bearing angle with 57Δ Fresnel horizontal peripheral prisms.

Video 3, available at http://links.lww.com/OPX/A537: dynamic video depiction: simulated walking with a colliding pedestrian at 15° bearing angle with 57Δ Fresnel oblique peripheral prisms.

Video 4, available at http://links.lww.com/OPX/A538: dynamic video depiction: simulated walking with a colliding pedestrian at 30° bearing angle with 57Δ Fresnel oblique peripheral prisms.

Submitted: January 28, 2021

Accepted: May 24, 2021

Funding/Support: National Eye Institute (R01-EY30777; to J-HJ); National Eye Institute (R01-EY23385; to EP); and National Eye Institute (P30-EY003790).

Conflict of Interest Disclosure: Coauthor EP has a patent for the peripheral prisms, assigned to the Schepens Eye Research Institute and licensed to Chadwick Optical, Inc. EP also has a patent application for the multiperiscopic prisms, assigned to the Schepens Eye Research Institute.

Author Contributions and Acknowledgments: Conceptualization: J-HJ; Data Curation: J-HJ, NMK; Formal Analysis: J-HJ; Funding Acquisition: J-HJ, EP; Investigation: J-HJ; Methodology: J-HJ, NMK; Project Administration: J-HJ, EP; Resources: J-HJ, EP; Software: J-HJ; Supervision: J-HJ, EP; Validation: J-HJ, NMK; Visualization: J-HJ, NMK; Writing – Original Draft: J-HJ; Writing – Review & Editing: J-HJ, NMK, EP.

Supported in part by the National Institutes of Health grants R01-EY30777 (J-HJ), EY23385 (EP), and P30-EY003790 (Schepens Eye Research Institute).

The authors thank Mr. Kenny Tang, Ms. Manda, and Dr. Mojtaba Falahati for their help with the preparation of figures.

REFERENCES

1. Levin M, Kelleher DK. Driving with a Bioptic Telescope: An Interdisciplinary Approach. Am J Optom Physiol Opt 1975;52:200–6.

2. Feinbloom W. Driving with Bioptic Telescopic Spectacles (BTS). Am J Optom Physiol Opt 1977;54:35–42.

3. Jose R, Browning R. Designing a Bioptic-contact Lens Telescopic System. Am J Optom Physiol Opt 1983; 60:74–9.

4. Greene HA, Pekar J. Bioptic Telescope Utilization Survey. J Vis Rehab 1987;1:39–48.

5. Nguyen A, Nguyen AT, Hemenger RP, et al. Resolution, Field of View, and Retinal Illuminance of Miniaturized Bioptic Telescopes and Their Clinical Significance. J Vis Rehab 1993;7:5–9.

6. Fetchenheuer I, Peli E, Woods RL. Functional Visual Fields of Monocular Bioptic Telescopes (Abstract). Activity and Participation: The 7th International Conference on Low Vision; Göteborg, Sweden; July 21–25, 2002.

7. Kozlowski JM, Jalkh AE. An Improved Negative-lens Field Expander for Patients with Concentric Field Constriction. Arch Ophthalmol 1985;103:326.

8. Drasdo N. Visual Field Expanders. Am J Optom Physiol Opt 1976;53(9 Pt. 1):464–7.

9. Mehr EB, Quillman RD. Field "Expansion" by Use of Binocular Full-field Reversed 1.3× Telescopic Spectacles: A Case Report. Am J Optom Physiol Opt 1979; 56:446–50.

10. Szlyk JP, Seiple W, Laderman DJ, et al. Use of Bioptic Amorphic Lenses to Expand the Visual Field in Patients with Peripheral Loss. Optom Vis Sci 1998; 75:518–24.

11. Goodlaw E. Review of Low Vision Management of Visual Field Defects. Optom Monthly 1983;74:363–8.

12. Cohen JM. An Overview of Enhancement Techniques for Peripheral Field Loss. J Am Optom Assoc 1993;64:60–70.

13. Peli E. Field Expansion for Homonymous Hemianopia by Optically-induced Peripheral Exotropia. Optom Vis Sci 2000;77:453–64.

14. Peli E, Vargas-Martin F, Kurukuti NM, et al. Multiperiscopic Prism Device for Field Expansion. Biomed Opt Express 2020;11:4872–89.

15. Apfelbaum H, Peli E. Tunnel Vision Prismatic Field Expansion: Challenges and Requirements. Transl Vis Sci Technol 2015;4:8.

16. Jose R, Ousley BA. The Visually Handicapped, Driving with Bioptics—Some New Facts. Rehabil Optom 1984;2:2–5.

17. Fonda G. Bioptic Telescopic Spectacle Is a Hazard for Operating a Motor Vehicle. Arch Ophthalmol 1983; 101:1907–8.

18. Apfelbaum HL, Ross NC, Bowers AR, et al. Considering Apical Scotomas, Confusion, and Diplopia when Prescribing Prisms for Homonymous Hemianopia. Transl Vis Sci Technol 2013;2:2.

19. Harrington DO, Drake MV. The Visual Fields: Text and Atlas of Clinical Perimetry. 6th ed. London, United Kingdom: Mosby; 1990.

20. Choplin NT, Edwards RP. Visual Fields. Thorofare, NJ: SLACK Inc.; 1998.

21. Jung JH, Peli E. Field Expansion for Acquired Monocular Vision Using a Multiplexing Prism. Optom Vis Sci 2018;95:814–28.

22. Good GW, Fogt N, Daum KM, et al. Dynamic Visual Fields of One-eyed Observers. Optometry 2005;76: 285–92.

23. Jung JH, Peli E. Impact of High Power and Angle of Incidence on Prism Corrections for Visual Field Loss. Opt Eng 2014;53:10.1117/1.OE.53.6.061707.

24. Welsh RC. The Roving Ring Scotomz: With Its Jack-in-the-box Phenomenon of Strong-plus (Aphakic) Spectacle Lenses. Am J Ophthalmol 1961;51:1277–81.

25. Peli E, Vargas-Martin F. In-the-spectacle-lens Telescopic Device. J Biomed Opt 2008;13:1–11.

26. Doherty AL, Bowers AR, Luo G, et al. Object Detection in the Ring Scotoma of a Monocular Bioptic Telescope. Arch Ophthalmol 2011;129:611–7.

27. Dille JR, Marano JA. The Effects of Spectacle Frames on Field of Vision. Aviat Space Environ Med 1984;55:957–9.

28. Woods RL, Fetchenheuer I, Vargas-Martin F, et al. The Impact of Non-immersive Head-mounted Displays (HMD) on the Visual Field. J Soc Inf Disp 2003;11:191–8.

29. Ogle K. Distortion of the Image by Prisms. J Opt Soc Am 1951;41:1023–8.

30. Ogle K. Distortion of the Image by Ophthalmic Prisms. AMA Arch Ophthalmol 1952;47:121–1.

31. Katz M. Visual Acuity through Fresnel, Refractive, and Hybrid Diffractive/Refractive Prisms. Optometry 2004;75:503–8.

32. Katz M. Contrast Sensitivity through Hybrid Diffractive, Fresnel, and Refractive Prisms. Optometry 2004;75: 509–16.

33. Choi HJ, Peli E, Park M, et al. Design of 45° Periscopic Visual Field Expansion Device for Peripheral Field Loss. Opt Commun 2020;454:124364.

34. Peli E, Jung JH. Multiplexing Prisms for Field Expansion. Optom Vis Sci 2017;94:817–29.

35. Tremblay EJ, Beer RD, Arianpour A, et al. Telescopic Vision Contact Lens. Proc SPIE 7885, Ophthalmic Technologies XXI 2011;788510:1–8.

36. Tremblay EJ, Stamenov I, Beer RD, et al. Switchable Telescopic Contact Lens. Opt Express 2013;21:15980–6.

37. Arianpour A, Schuster GM, Tremblay EJ, et al. Wearable Telescopic Contact Lens. Appl Optics 2015;54: 7195–204.

38. Bailey IL. Can Prisms Control Eccentric Viewing? Optom Monthly 1983;74:360–2.

39. Vargas MF. Survey of a Free Cost View Finder for Visual Field Expansion. Int Congr Ser 2005;1282:1080–4.

40. Littlefield R. Theory of the "No-parallax" Point in Panorama Photography; 2015. Available at: https://www.janrik.net/PanoPostings/NoParallaxPoint/TheoryOfTheNoParallaxPoint.pdf. Accessed August 13, 2021.

41. Johnson RB. Correctly Making Panoramic Imagery and the Meaning of Optical Center. Proc SPIE 7060, Current Developments in Lens Design and Optical Engineering IX 2008;70600F:1–8.

42. Riggs LA, Tulunay SU. Visual Effects of Varying the Extent of Compensation for Eye Movements. J Opt Soc Am 1959;49:741–5.

43. Gross H, Blechinger F, Achtner B. Human Eye. In: Gross H, ed. Handbook of Optical Systems, Vol. 4: Survey of Optical Instruments. Weinheim, Germany: Wiley-VCH Verlag GmBH & Co.; 2008:1–45.

44. Jung JH, Castle R, Kurukuti NM, et al. Field Expansion with Multiplexing Prism Glasses Improves Pedestrian Detection for Acquired Monocular Vision. Transl Vis Sci Technol 2020;9:35.

45. Steptoe W. AR-Rift: Aligning Tracking and Video Spaces (Part 5). Available at: https://willsteptoe.com/post/67401705548/ar-rift-aligning-tracking-and-video-spaces-part-5. Accessed April 20, 2021.

46. Ocutech Inc. Fitting and Prescribing the Ocutech VES Mini; 2015. Available at: https://www.youtube.com/watch?v=phLKnpLOo2w. Accessed August 13, 2021.

47. Peli E, Bowers AR, Keeney K, et al. High-power Prismatic Devices for Oblique Peripheral Prisms. Optom Vis Sci 2016;93:521–33.

48. Stockman A, Sharpe L. Into the Twilight Zone: The Complexities of Mesopic Vision and Luminous Efficiency. Ophthalmic Physiol Opt 2006;26:225–39.

49. Charman WN. The Charles F. Prentice Award Lecture 2005: Optics of the Human Eye: Progress and Problems. Optom Vis Sci 2006;83:335–45.

50. Katz M, Citek K, Price I. Optical Properties of Low Vision Telescopes. J Am Optom Assoc 1987;58:320–31.

51. Peli E, Apfelbaum H, Berson EL, et al. The Risk of Pedestrian Collisions with Peripheral Visual Field Loss. J Vis 2016;16(15):5.

52. Qiu C, Jung JH, Tuccar-Burak M, et al. Measuring Pedestrian Collision Detection with Peripheral Field Loss and the Impact of Peripheral Prisms. Transl Vis Sci Technol 2018;7(5):1.

53. Lippmann O, Corn AL, Lewis MC. Bioptic Telescopic Spectacles and Driving Performance: A Study in Texas. J Vis Impair Blind 1988;82:182–7.

54. Corn AL, Lippmann O, Lewis MC. Licensed Drivers with Bioptic Telescopic Spectacles: User Profiles and Perceptions. RE:view 1990;21:221–30.

55. Gottlieb DD. Living with Vision Loss. Atlanta, GA: St. Barthelemy Press, Ltd.; 1996.

56. Dickinson C. Low Vision: Principles and Practice. Oxford, United Kingdom: Butterworth; 1998.

57. Fonda G. Approach Magnification Is Safer Than Bioptic Telescopic Spectacles for Operating a Motor Vehicle. Trans Pa Acad Ophthalmol Otolaryngol 1982; 35:137–40.

58. Doherty AL, Peli E, Luo G. Hazard Detection with a Monocular Bioptic Telescope. Ophthalmic Physiol Opt 2015;35:530–9.

59. Fonda G. Evaluation of the Honey Bee Lens. Arch Ophthalmol 1985;103:180–1.

60. Brilliant RL, Appel SD, Ruggiero RJ. The Amorphic Fresnel Prism Trioptical System. In: Woo GC, ed. Low Vision. New York, NY: Springer; 1987:209–15.

61. Peli E, Lipshitz I, Dotan G. Implantable Miniaturized Telescope (IMT) for Low Vision. In: Stuen C, Arditi A, Horowitz A, et al, eds. Vision Rehabilitation: Assessment, Intervention and Outcomes. Lisse, the Netherlands: Swets & Zeitlinger; 2000:200–3.

62. Luo G, Vargas-Martin F, Peli E. The Role of Peripheral Vision in Saccade Planning: Learning from People with Tunnel Vision. J Vis 2008;8:25.1–8.

63. Demer JL, Porter FI, Goldberg J, et al. Adaptation to Telescopic Spectacles: Vestibulo-ocular Reflex Plasticity. Invest Ophthalmol Vis Sci 1989;30:159–70.

64. Demer JL, Amjadi F. Dynamic Visual Acuity of Normal Subjects during Vertical Optotype and Head Motion. Invest Ophthalmol Vis Sci 1993;34:1894–906.

65. Ross NC, Bowers AR, Peli E. Peripheral Prism Glasses: Effects of Dominance, Suppression, and Background. Optom Vis Sci 2012;89:1343–52.

66. Haun A, Peli E. Binocular Rivalry with Peripheral Prisms for Treatment of Hemianopia. J Vis 2012;12:211.

67. Shen J, Peli E, Bowers AR. Peripheral Prism Glasses: Effects of Moving and Stationary Backgrounds. Optom Vis Sci 2015;92:412–20.

68. Cheng D, Woo GC. The Effect of Conventional CR39 and Fresnel Prisms on High and Low Contrast Acuity. Ophthalmic Physiol Opt 2001;21:312–6.

69. Matthis JS, Yates JL, Hayhoe MM. Gaze and the Control of Foot Placement when Walking in Natural Terrain. Curr Biol 2018;28:1224–33.e5.

70. Peli E, inventor; Schepens Eye Research Institute, assignee. Peripheral Field Expansion Device. US Patent 7,374,284 B2. May 20, 2008.

71. Houston KE, Peli E, Goldstein RB, et al. Driving with Hemianopia VI: Peripheral Prisms and Perceptual-motor Training Improve Detection in a Driving Simulator. Transl Vis Sci Technol 2018;7(1):5.

72. Geisler WS, Perry JS. Real-time Simulation of Arbitrary Visual Fields. Proceeding of the ACM Symposium on Eye Tracking Research & Applications; 2002:83–7.

73. Peli E, Yang J, Goldstein RB. Image Invariance with Changes in Size: The Role of Peripheral Contrast Thresholds. J Opt Soc Am (A) 1991;8:1762–74.

74. Peli E. Contrast in Complex Images. J Opt Soc Am (A) 1990;7:2032–40.

75. Crabb DP, Smith ND, Glen FC, et al. How Does Glaucoma Look? Patient Perception of Visual Field Loss. Ophthalmology 2013;120:1120–6.

76. Taylor DJ, Edwards LA, Binns AM, et al. Seeing It Differently: Self-reported Description of Vision Loss in Dry Age-related Macular Degeneration. Ophthalmic Physiol Opt 2017;38:98–105.